FIELD MEASUREMENTS ON THE MILAN SUPERCONDUCTING MODEL MAGNET

E. Acerbi, G. Bellomo, C. Birattari, M. Castiglioni, C. De Martinis, E. Fabrici, L. Grillo, F. Resmini, A. Salomone**

Introduction

In this paper we shall report the results of extensive magnetic field measurements carried out on the Milan 1:6 model magnet. This activity involved a period of about 8 months, from May 1977 to January 1978.

The main purpose of the magnetic field studies on the model was not so much to obtain a precise and definitive pole tip configuration which would later be used on the real machine. This was in fact deemed premature at such an early stage of the project. Rather, our main goal was to assess the validity of the theoretical calculations made for the magnet and to understand their limits.

Every effort was of course made to obtain a pole tip geometry which would be as close as possible to a "realistic" cyclotron geometry, but nevertheless the data obtained and the discussion of the results should be looked at in the perspective just outlined above.

The field measuring apparatus has been fully described in ref. (1), and therefore, we do not deem it necessary to go in any detail here. Let us just comment that no troubles arose with either the polar grid positioning system used for internal radii up to the pole diameter of 15 cm, or with the cartesian coordinate positioning device used for mapping fringing fields. Also the three Hall plates, Siemens SBV-585-S1, spaced at 5 mm radial intervals, and simultaneously employed in all field mappings, performed very satisfactorily. The overall errors in the measurements, when all factors are taken into account, are no larger than ±0.05%.

Pole Tip Geometry

Although three different pole geometries have been investigated at various times, conventionally named A0, A1, A2, they varied only in the radial profile of hills and valleys, while major characteristics remained constant. Accordingly, and since the largest part of the data was taken with A2 geometry, in the following we shall mostly concern ourselves with the latter. A schematic view of this geometry is presented in fig. 1. Pole radius is 15 cm, and the spiral constants of the hill edges are 9.6 and 10.8 m^{-1}. The holes in the valleys of 17 mm and 41.6 mm in diameter simulate those needed for R.F. trimming capacitors and R.F. stems respectively, while the central hole, 25 mm in diameter, simulates the ion source hole. Radial profiles of hill and valley are shown in detail in fig. 2. This profile was intended to give an average field smoothly decreasing as a function of radius, as we expect it to be in the real machine.

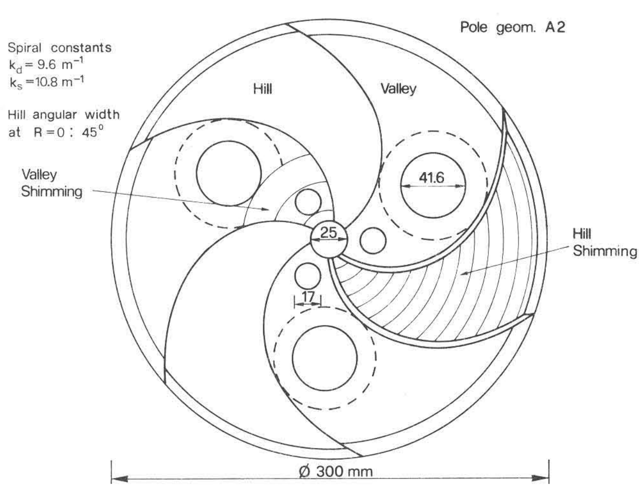

Fig. 1 - Plan of the pole tip geometry.

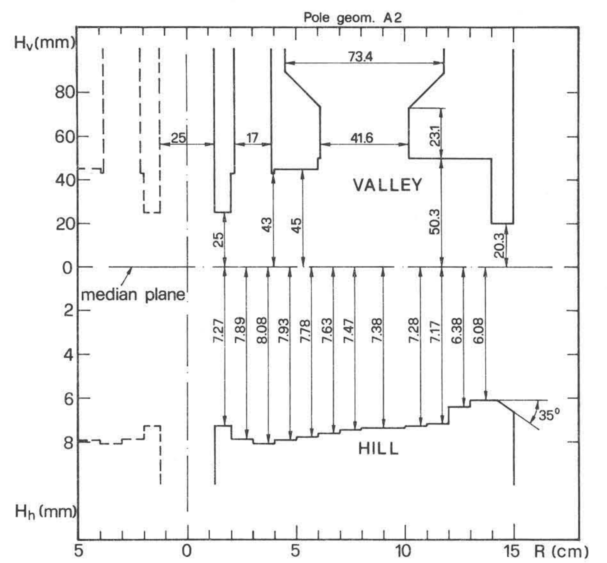

Fig. 2 - Hills and valleys radial profiles.

Summary of Field Maps

Before entering a detailed discussion of the data, it is perhaps useful to summarize briefly the magnetic field measuring runs which we have available. This is done in Table I, where excitation currents at which maps were taken and the type of maps available are listed.

Table I

Available magnetic field maps. (Pole geometry A2)

I (A)	IN (At) x 10^6	$\bar{B}$ (kG) at R=7.5 cm	Azimuthal span	Fringing field map
15.03	.1032	14.40	120°	no
25.00	.1716	16.80	120°	no
39.70	.2726	20.00	120°	no
60.25	.4137	24.25	120°	no
80.18	.5505	28.40	360°	yes
100.07	.6871	32.00	120°	no
119.25	.8188	35.65	360°	yes

Given the amount of data, it is perhaps more useful to present them according to the following three major topics, as far as magnetic field properties are concerned, namely: a) Field modulation; b) Average magnetic behaviour; c) Field imperfections.

Azimuthal Field Modulation

As already reported(1) the experimental field modulation is very close to the one expected from saturated

**University of Milan and Istituto Nazionale di Fisica Nucleare - INFN - Milan - Italy.

0018-9499/79/0400-2114$00.75

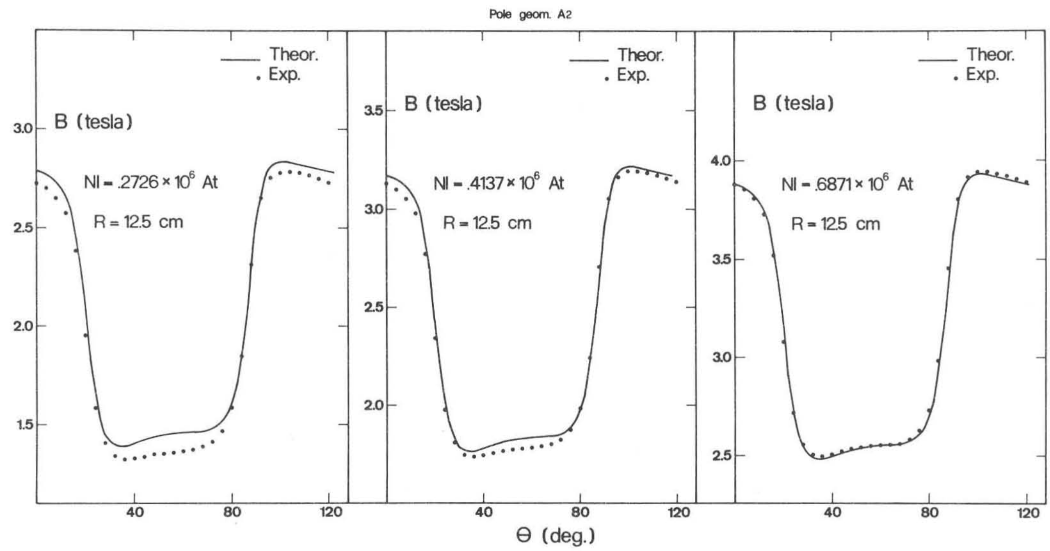

Fig. 3 - Field modulation, at 12.5 cm radius, for three different coil excitations.

pole tips, an assumption used throughout in our calculations,(2) with M_{sat} = 2.16 T. An example of field modulation over 120° at a radius of 12.5 cm and at 3 different coil excitations is shown in fig. 3. It can be recognized that although the agreement of absolute values with the calculations is somewhat less satisfactory at lower excitations, due to the difficulty of exactly calculating the average field, the three field waves are essentially identical, and in fact they can be superposed, if the average fields are properly shifted as indicated in the figure.

An important quantity relevant to field modulation is the flutter, which is shown in fig. 4 as a function of radius, again for three different coil excitation levels. The calculated values would practically coincide with the experimental points, should also the calculated value of the average magnetic field be coincident, an argument to which we shall turn presently.

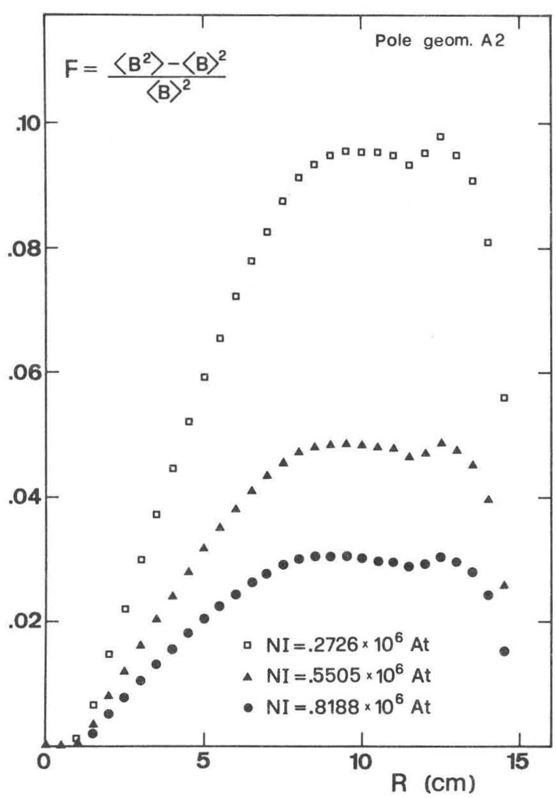

Fig. 4 - Flutter, as a function of radius, at the three field levels indicated.

Average Magnetic Field Behaviour

The varying degree of saturation of the pole and the yoke makes it rather difficult to predict exactly the value of the average magnetic field. The latter can be thought of, at least in first approximation, as the sum of three contributions: i) coil field, ii) saturated pole tip field, iii) "yoke" contribution. It is this last one which is the most difficult to calculate, especially in a true three dimensional problem like the present one. Although codes like POISSON and TRIM (see ref. (3)) can be employed in the case of cylindrical symmetries, we have not made a large effort in this direction, because our unsymmetrical yoke(4) prevents a straightforward use of these codes for a realistic case. In most cases we have preferred the method of image currents, whose details are now briefly reviewed.

The yoke magnetic field is assumed to be given by a current flowing in coils which are the mirror images of the "true" coils with respect to the upper and lower surfaces of the yoke. This current may be written as:

$$I = I_0 (\mu_r - 1)/(\mu_r + 1)$$

where I_0 and μ_r are respectively the "true" coil current and the relative permeability of the yoke iron. For each excitation current I_0, the quantity μ_r is evaluated as a function of the magnetic field B in the yoke, on the assumption of no missing flux.

The average magnetic fields $\overline{B}(R)$, both experimental and calculated, are presented in fig. 5 at five different coil excitations as a function of radius. Let us note that the lowest excitation level presented here (.2726 10^6 At) corresponds to an average field around 20 kG, and therefore too low to be used in the real machine. It does help, nevertheless, in understanding the general trend of the data. At low levels, the calculation usually overestimates the field by ∿ .4 - .5 kG. It is very much consistent, to less than 1%, in the intermediate range (24 to 30 kG), and thereafter underestimates the field by increasing amounts (∿ 2% at 35 kG).

0018-9499/79/0400-2115$00.75 ©1979 IEEE

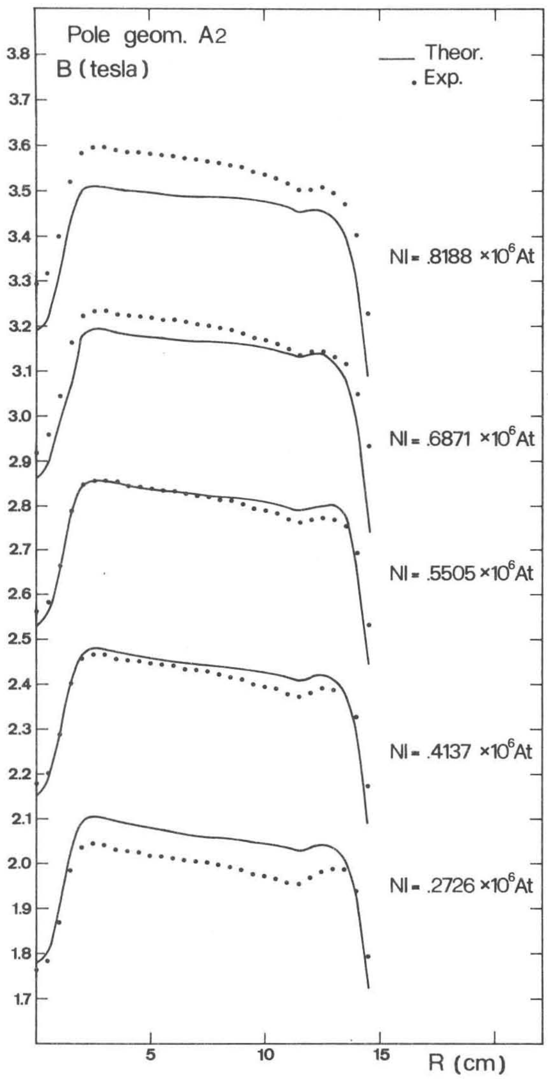

Fig. 5 - Experimental and calculated magnetic fields as a function of R, for five different coil excitations. See text for details.

This obviously suggests that the total iron-produced magnetic field (pole tips plus "yoke") is not at all constant, even in a fully saturated pole tip situation, but does vary as a function of the average field level. This behaviour is very clearly indicated in fig. 6, where the contribution from the coils has been subtracted from the experimental magnetic field for every coil excitation shown. The figure thus presents the average field actually produced by the entire iron configuration, at the different field levels. It can be noted that, apart from the very low excitation cases (curves E and D), where also a sensible slope variation is present, the average field moves up, with increasing coil excitation, by as much as $\sim$ 2 kG. The calculations, as was shown in fig. 5, can account for about 60% of this variation. However, the remaining discrepancy should not be considered as very important, because it mostly reflects itself in a different coil current for producing a given average field.

Fringing field behaviour follows a similar trend. Experimental data for the fringing field, as a function of radius, are presented in figs. 7 and 8 for two azimuths corresponding to a hill and a valley region,

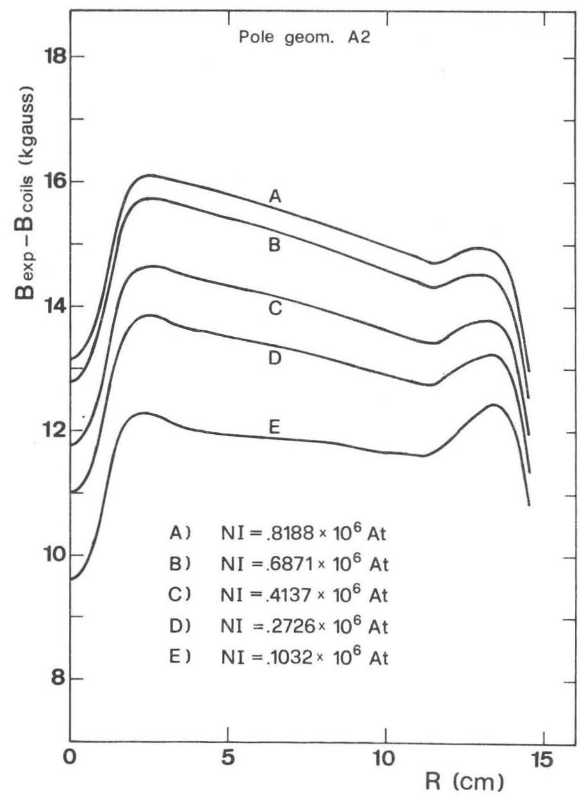

Fig. 6 - Experimental average magnetic field (contribution from the coils subtracted) produced by the iron configuration alone, at various coil excitations.

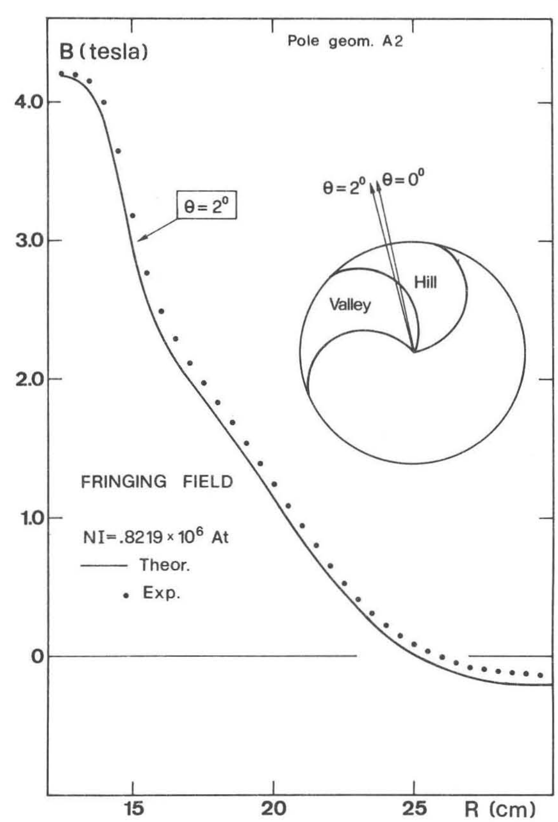

Fig. 7 - Experimental and calculated fringing field, as a function of radius, across a hill at .8219 10^6 At.

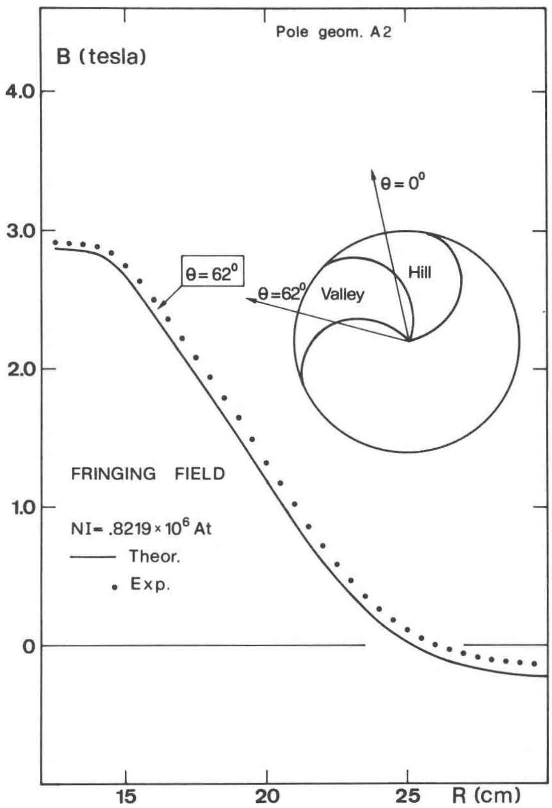

Fig. 8 - Experimental and calculated fringing field, as a function of radius, across a valley, at .8219 10^6 At.

respectively. The field slope is exactly reproduced, while the level is in both cases underestimated by about .8 kG.

Field Imperfections

Since first harmonic imperfections coming from coil mispositionings, i.e. construction errors, are already discussed in ref. (4), we shall just discuss here field imperfections arising from our peculiar yoke geometry. Its fourfold symmetry should result in the appearance of a 4^{th} and perhaps 8^{th} harmonic in the field, and indeed they are both observed as shown in fig. 9. The maximum amplitude of the 4^{th} harmonic is about 40 G, at .82 10^6 At, and that of the 8^{th} about 15 G. No effort has, however, been made to predict these amplitudes from field calculations, since the uncertainties previously discussed are really too large to allow realistic calculations of such small effects.

Summary

As a whole, we believe that, as far as magnetic field properties are concerned, the following conclusions can be drawn with a large degree of assurance:

i) azimuthal field modulation, as calculated from any saturated pole tip geometry, agrees with data to such an extent that this method can safely be used to predict harmonic amplitudes and phases;

ii) absolute values of the average magnetic field can be predicted, even with a rather rough approximation, to within ± 1.%, at least in the range of fields $B \geq 25$ kG where pole iron is largely saturated. This holds for inner radii fields and fringing fields as well;

iii) more refined and time-consuming calculations can probably trim down these errors to a few parts per thousand, although, in our belief, with little more advantage from the point of view of a cyclotron early design.

As quoted above, all magnetic field measurements stopped in January 1978. They will resume only if the cyclotron will be built, this time with the precise purpose of designing the final iron geometry of the machine. We believe that the availability of the model will enable us to shorten considerably the time needed to define, down to the very last details, the overall structure of the cyclotron.

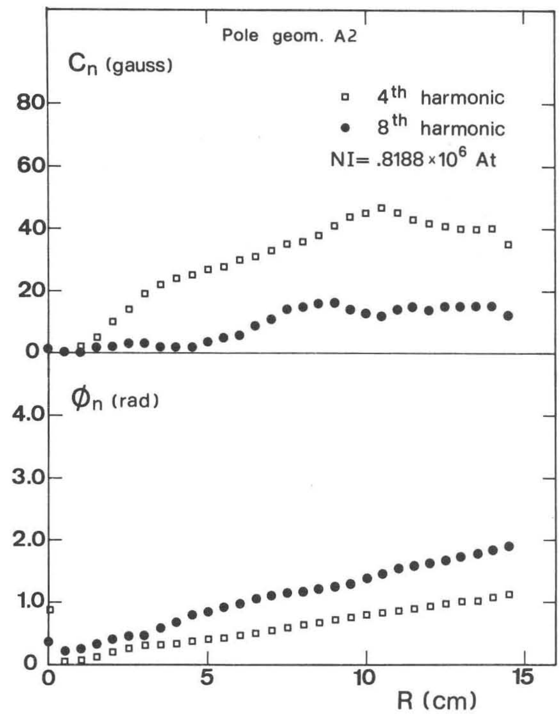

Fig. 9 - Amplitudes and phases of 4^{th} and 8^{th} harmonics of the field, as a function of radius.

References

1) E. Acerbi, G. Bellomo, C. Birattari, M. Castiglioni, C. De Martinis, E. Fabrici, L. Grillo, F. Resmini; Magnetic Field Measuring System for a Small Gap Superconducting Magnet; Proceed. of Magnet Conference - Bratislave (1978).
2) E. Acerbi, G. Bellomo, M. Castiglioni, C. De Martinis, E. Fabrici; Magnetic Field Calculations for a Proposed Superconducting Cyclotron at the University of Milan; IEEE Trans. NS-24 (3), 1168 (1977).
3) S.J. Colonias; Particle Accelerators Design: Computer Programs; Academic Press, N.Y.
4) E. Acerbi, G. Bellomo, M. Castiglioni, C. De Martinis, E. Fabrici, C. Pagani, F. Resmini; Model Studies for the Superconducting Cyclotron Project in Milan; Proceed. of this Conference.